Podocalyxin is required for maintaining blood–brain barrier function during acute inflammation

Jessica Cait[a], Michael R. Hughes[a,1], Matthew R. Zeglinski[b,c,d], Allen W. Chan[e,f,g,h,i], Sabrina Osterhof[a], R. Wilder Scott[a,j], Diana Canals Hernaez[a], Alissa Cait[a], A. Wayne Vogl[j,k], Pascal Bernatchez[d,l], T. Michael Underhill[a,j], David J. Granville[b,c,d], Timothy H. Murphy[e,f,g], Calvin D. Roskelley[j,k], and Kelly M. McNagny[a,1]

[a]Biomedical Research Centre, University of British Columbia, Vancouver, BC, Canada V6T 1Z3; [b]ICORD Centre, University of British Columbia, Vancouver, BC, Canada V5Z 1M9; [c]Department of Pathology and Laboratory Medicine, University of British Columbia, Vancouver, BC, Canada V6T 2B5; [d]Centre for Heart and Lung Innovation, St Paul's Hospital, Vancouver, BC, Canada V6Z 1Y6; [e]Department of Psychiatry, University of British Columbia, Vancouver, BC, Canada V6T 2A1; [f]Kinsmen Laboratory of Neurological Research, University of British Columbia, Vancouver, BC, Canada V6T 1Z4; [g]Djavad Mowafaghian Center for Brain Health, University of British Columbia, Vancouver, BC, Canada V6T 1Z3; [h]Neuroscience and Mental Health Institute, University of Alberta, Edmonton, AB, Canada T6G 2R3; [i]Neurochemical Research Unit, Department of Psychiatry, Faculty of Medicine and Dentistry, University of Alberta, Edmonton, AB, Canada T6G 2R3; [j]Department of Cellular and Physiological Sciences, University of British Columbia, Vancouver, BC, Canada V6T 1Z4; [k]Life Sciences Institute, University of British Columbia, Vancouver, BC, Canada V6T 1Z4; and [l]Department of Anaesthesiology, Pharmacology & Therapeutics, University of British Columbia, Vancouver, BC, Canada V6T 1Z3

Edited by Lawrence Steinman, Stanford University School of Medicine, Stanford, CA, and approved January 15, 2019 (received for review September 6, 2018)

Podocalyxin (Podxl) is broadly expressed on the luminal face of most blood vessels in adult vertebrates, yet its function on these cells is poorly defined. In the present study, we identified specific functions for Podxl in maintaining endothelial barrier function. Using electrical cell substrate impedance sensing and live imaging, we found that, in the absence of Podxl, human umbilical vein endothelial cells fail to form an efficient barrier when plated on several extracellular matrix substrates. In addition, these monolayers lack adherens junctions and focal adhesions and display a disorganized cortical actin cytoskeleton. Thus, Podxl has a key role in promoting the appropriate endothelial morphogenesis required to form functional barriers. This conclusion is further supported by analyses of mutant mice in which we conditionally deleted a floxed allele of *Podxl* in vascular endothelial cells (vECs) using Tie2Cre mice (*Podxl*$^{\Delta Tie2Cre}$). Although we did not detect substantially altered permeability in naïve mice, systemic priming with lipopolysaccharide (LPS) selectively disrupted the blood–brain barrier (BBB) in *Podxl*$^{\Delta Tie2Cre}$ mice. To study the potential consequence of this BBB breach, we used a selective agonist (TFLLR-NH_2) of the protease-activated receptor-1 (PAR-1), a thrombin receptor expressed by vECs, neuronal cells, and glial cells. In response to systemic administration of TFLLR-NH_2, LPS-primed *Podxl*$^{\Delta Tie2Cre}$ mice become completely immobilized for a 5-min period, coinciding with severely dampened neuroelectric activity. We conclude that Podxl expression by CNS tissue vECs is essential for BBB maintenance under inflammatory conditions.

blood–brain barrier | podocalyxin | endothelial | barrier function | CD34 family

The blood vessel wall serves as a selective, semipermeable barrier separating blood constituents from tissue parenchyma. The junctional interactions between neighboring vascular endothelial cells (vECs), their adhesion to the basement membrane, and the apical/luminal glycocalyx all contribute to barrier architecture and function (1–3). Maintenance of this barrier is particularly crucial in the central nervous system (CNS) to prevent exposure of this highly sensitive neural tissue to endogenous plasma constituents, inflammatory cells, and exogenous toxins. The blood–brain barrier (BBB) is supported by a neurovascular unit consisting of neurons, pericytes, CNS glial cells (astrocytes and microglia), and specialized vascular endothelia that form both tight junctions (TJs) and adherens junctions (AJs) between adjacent vECs.

The actin cytoskeleton of endothelial cells in the BBB is intimately associated with several key junctional proteins (4). In response to tissue injury, disassembly of the actin cytoskeleton disrupts junctional complexes and promotes degradation and internalization of these proteins, leading ultimately to disruption of the endothelial barrier (5) and recruitment of immune cells and plasma factors to effect repair. Some of the plasma components that affect this repair include active proteases, such as thrombin. Thus, barrier remodeling has a central role in the normal repair of injured tissues, as well as in the pathogenesis of inflammatory and vascular diseases, including stroke and traumatic brain injury (6).

Podocalyxin (Podxl) is a CD34-family sialomucin expressed primarily by vascular endothelia and kidney podocytes in adult vertebrates. It is also expressed by rare stem cell populations of several tissues (7) and stress erythroid progenitors (8, 9) and is aberrantly expressed in aggressive carcinomas, glioblastoma, blood cancers, and germ cell tumors (10, 11). Podxl was originally identified as the predominant sialoglycoprotein in kidney podocytes, where by virtue of its strong negatively charged mucin domain, it was postulated to play a role in urine filtration (12, 13). Subsequent gene deletion studies in mice showed that Podxl plays an essential role in podocyte morphogenesis; in the absence of Podxl expression, immature podocytes retain AJs and TJs, leading to anuria and perinatal lethality (14, 15). In addition, we and others have shown that Podxl has the capacity to

Significance

This article demonstrates a role for podocalyxin in blood–brain barrier (BBB) function. Podocalyxin expression on endothelial cells promotes the formation of adhesion interactions and barrier formation. Furthermore, it describes a neuroelectric phenotype elicited by a selective protease-activated receptor-1 (PAR-1) agonist. PAR-1 activation by serum proteases (e.g., thrombin) leaking into the central nervous system during inflammation has the potential to impact the course of brain injury and recovery. However, the role of PAR-1 in the pathophysiology of neuroinflammation is poorly understood. In summary, this study offers unique insight into the impact of PAR-1 activation in neuroinflammation and implicates podocalyxin as a therapeutic target for the manipulation of BBB permeability and the treatment of neurodegenerative disease.

Author contributions: J.C., M.R.H., A.W.C., T.H.M., C.D.R., and K.M.M. designed research; J.C., M.R.H., M.R.Z., A.W.C., S.O., R.W.S., D.C.H., A.C., and A.W.V. performed research; P.B., T.M.U., D.J.G., and T.H.M. contributed new reagents/analytic tools; J.C., M.R.H., M.R.Z., and A.W.C. analyzed data; and J.C., M.R.H., and K.M.M. wrote the paper.

The authors declare no conflict of interest.

This article is a PNAS Direct Submission.

[1]To whom correspondence may be addressed. Email: mhughes@brc.ubc.ca or kelly@brc.ubc.ca.

This article contains supporting information online at www.pnas.org/lookup/suppl/doi:10.1073/pnas.1814766116/-/DCSupplemental.

Published online February 20, 2019.

regulate integrin function in polarized epithelial cells (16, 17). Normally, Podxl is potently targeted to the apical domains of epithelial cells during cell polarization and, in its absence, integrin sorting to basolateral domains is attenuated. Thus, although this apical sialomucin does not function as an adhesion molecule per se, its expression, or lack thereof, can dramatically alter the adhesive properties of cells.

Although Podxl and its close relative, CD34, are highly expressed by all adult vascular endothelial cells (vECs), little is known of their function on these cells. We previously found that primary *Podxl*-null vECs isolated from mouse lungs have impaired ability to spread on laminin, a major component of the basal extracellular matrix (ECM), in vitro, as well as an altered expression pattern of integrins and matrix proteins. Nevertheless, mice lacking Podxl on lung vECs display only a modest increase in lung vascular permeability and exhibit no other overt defects at steady state (18). Importantly, due to the tissue-specificity of the vascular Cre-deleter strain (Cdh5Cre) we used in these previous studies, *Podxl* was not deleted in CNS vascular beds, a tissue that is notable for possessing the highest levels of *Podxl* expression on endothelia (19).

In the present study, we performed a thorough analysis of the effects of Podxl loss in primary human endothelial cells in vitro and used a more widely effective Cre-deleter strain to assess how *Podxl* expression regulates mouse BBB integrity in vivo. We found that Podxl is required for human endothelial cells to assemble a functional barrier on multiple extracellular matrices, and that its loss leads to disruptions in filamentous actin (F-actin)-dependent cytoskeletal rearrangement, AJ formation, and formation of focal adhesions (FAs). Correspondingly, we found that in vivo, Podxl maintains the integrity of the BBB during acute inflammation. Its loss in $Podxl^{\Delta Tie2Cre}$ mice leads to BBB dysfunction in response to inflammation, exposure of neurons and glial cells to plasma proteins, and, through this exposure, increased sensitivity to PAR-1 activation. We conclude that Podxl plays a critical role in matrix-dependent endothelial cell barrier integrity and appropriate function of the BBB.

Results

Podxl Is Required for Endothelial Morphogenesis. We previously found that primary *Podxl*-deficient mouse lung vECs have a spreading defect on laminin (17). To determine whether primary human endothelial cells similarly require Podxl for efficient spreading on ECM, we transiently transfected human umbilical vein endothelial cells (HUVECs) with a *PODXL*-targeting ($PODXL^{KD}$) or nontargeting control siRNA (*SI Appendix*, Fig. S1). We then seeded control and $PODXL^{KD}$ cells on plates coated with fibronectin, collagen, or laminin, the three principal ECM proteins detected in most tissues that serve as integrin-specific adhesive substrates in various physiological conditions (20). We monitored growth over several days using real-time video microscopy, fluorescence microscopy (on fixed cells at selected time points), and electric cell substrate impedance sensing (ECIS) (*SI Appendix*, Fig. S2). Control and $PODXL^{KD}$ cells adhere to and form what appear to be equally dense monolayers on all matrices in the first 24 h in culture (Fig. 1*A*). However, over the next 72 h, $PODXL^{KD}$ monolayers become progressively disorganized as the cells lose their ability to maintain appropriate spacing and cell–cell contacts (Fig. 1*A* and Movies S1–S6). Only control cells maintain a uniform monolayer after 42 h in culture (Fig. 1*B*). In contrast, at this time point, clusters of $PODXL^{KD}$ HUVECs fail to form normal cell–cell attachments and instead show gaps between neighboring cells regardless of the choice of matrix (Fig. 1*B*). No major differences in cell viability were observed in these cultures (*SI Appendix*, Fig. S3).

To better assess the interactions between cells, we stained fixed monolayers with an anti–VE-cadherin antibody after 48 h in culture, when $PODXL^{KD}$ and control HUVEC growth characteristics begin to diverge (Fig. 1*B*). While VE-cadherin was uniformly distributed at the cell–cell contacts in control cells plated on fibronectin, collagen, or laminin, VE-cadherin on $PODXL^{KD}$ HUVEC cultures was sparsely distributed at rare cell–cell contact sites (when present) and in most cells was localized to the cytosol (Fig. 1*B*). Correspondingly, fluorescence microscopy of DAPI- and phalloidin-stained monolayers at the 72-h time point revealed striking differences in the arrangement of the actin cytoskeleton and cell spreading (Fig. 2 and *SI Appendix*, Fig. S4*A*). Although control cells have a normal radial arrangement of polymerized actin and stress fibers, $PODXL^{KD}$ cells exhibit decreased stress fiber formation and nonuniform hair-like projections extending from the cell indicative of retraction fibers. Some $PODXL^{KD}$ cells have an irregular wavy actin appearance compared with the more linear actin fibers observed in the control cells. Furthermore, there is a decreased intensity of phalloidin staining in the $PODXL^{KD}$ cells, indicative of less total F-actin (Fig. 2 and *SI Appendix*, Fig. S4*B*).

Staining of control HUVECs for β-catenin revealed prominent localization of β-catenin to cell–cell contacts. In contrast, in $PODXL^{KD}$ HUVECs, β-catenin is located primarily in the cell nucleus—a result consistent with the lack of stable contribution to cell–cell contacts, aberrant AJ formation, and poor barrier formation in the absence of Podxl. Finally, we examined the ability of $PODXL^{KD}$ HUVECs to form focal adhesion (FA) contacts to matrix. Vinculin regulates and marks protein complexes that form FA (21). We observed clear, punctate vinculin staining at the peripheral cell membranes of control cells, whereas in $PODXL^{KD}$ cells, vinculin accumulates in perinuclear structures (Fig. 2). This disparate vinculin-staining pattern was observed for all matrices. This suggests that Podxl expression promotes FA complex formation in HUVECs bound to common ECM components. Intriguingly, assessment of overall vinculin protein expression (by measuring staining intensity) suggested that vinculin is expressed at higher levels in $PODXL^{KD}$ compared with control cells (*SI Appendix*, Fig. S4*C*). Thus, vinculin localization, rather than protein expression or stability, is aberrant in Podxl-deficient HUVECs.

In summary, Podxl promotes the formation of AJs between cells, organization of the cortical actin cytoskeleton, and generation of FA between cells and the ECM. We conclude that Podxl has a critical role in the regulation of endothelial cell architecture and matrix adhesion required to form a functional barrier.

Podxl Promotes Endothelial Cell Spreading and Optimal Barrier Function. We next assessed the role of Podxl in the establishment of an endothelial barrier using a real-time ECIS system. ECIS uses an alternating current across an electrode that is influenced by cells as they adhere and grow. Cells act as insulators, thereby increasing resistance across the electrode as they form a monolayer. At low frequencies (4 kHz), as cells form a confluent monolayer and a mature barrier, current flow between cells is reduced (high resistance) and can be used as a measure of barrier function. At high frequencies (64 kHz), current flow through cells is also reduced (low capacitance) and can be used as a measure of electrode coverage. Using these parameters, mathematical ECIS modeling provides a more detailed analysis of cell–cell (Rb) and cell–matrix (α) interactions (21, 22). Identical concentrations of Podxl-deficient $PODXL^{KD}$ and control HUVECs were plated on ECIS electrodes coated with selected matrix components: fibronectin, collagen, or laminin.

To assess cell coverage and barrier function, we measured capacitance at 64 kHz and resistance at 4 kHz (AC frequency, *f*), respectively, over the first 24 h of culture. When plated on laminin, *PODXL*-deficient HUVEC ($PODXL^{KD}$) display decreased electrode coverage, as shown by increased capacitance (f = 64 kHz) compared with controls (Fig. 3*A*). No significant difference in electrode coverage was observed when cells were

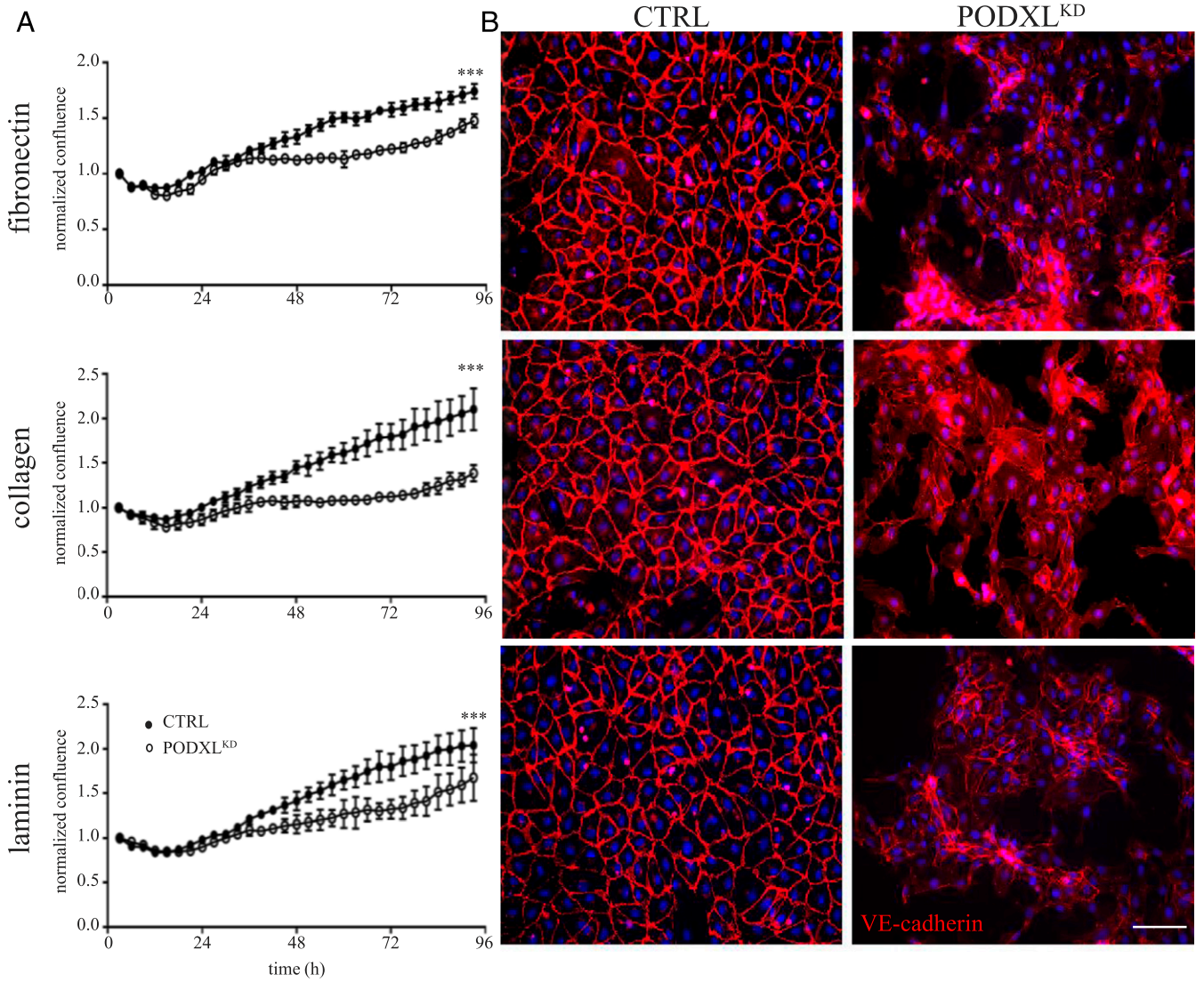

Fig. 1. Podxl promotes HUVEC monolayer formation. (*A*) Confluence normalized to starting concentration as measured by the IncuCyte ZOOM confluence processing analysis tool (basic analyzer). WT and PODXL^{KD} HUVEC monolayers measured over 96 h. Error bars represent SD (n = 3). ***Significantly less confluent than WT with $P < 0.001$ (determined by Student's t test). (*B*) VE-cadherin staining (red) of WT and PODXL^{KD} HUVECs at 48 h after seeding cells on the indicated matrix. DAPI (nuclear stain). (Scale bars: 100 μm.)

plated on fibronectin or collagen, suggesting that Podxl regulates matrix-specific cell spreading and adhesion functions in endothelial cells. In addition, PODXL^{KD} monolayers consistently exhibit reduced transendothelial resistance (f = 4 kHz) on all matrix components, indicative of defects in mature barrier formation (Fig. 3*B*). Impaired barrier function was most striking when PODXL^{KD} cells were plated on laminin-coated electrodes.

Using ECIS mathematical modeling, we separated the contributions of barrier function attributable to cell–cell interactions (Rb) and those attributable to cell–matrix interactions (α) (Fig. 3 *C* and *D*) (21). On all three matrices, PODXL^{KD} cells exhibit decreased Rb, indicative of poorly formed cell–cell interactions. In addition, although there was no significant difference when plated on fibronectin, when plated on laminin and collagen, the increased α parameter observed with PODXL^{KD} cells indicates impaired cell–matrix adhesion. We conclude that expression of Podxl is required for the efficient binding of HUVECs to the basal matrix, as well as the formation of cell–cell interactions essential to establishing optimal endothelial barrier function.

Podxl Is Required for Maintenance of BBB Integrity During Acute Systemic Inflammation. To further assess the role of Podxl in maintaining endothelial barrier function in vivo, we deleted Podxl in mouse vECs using two separate Cre-deleter strains, Cdh5Cre and Tie2Cre (23, 24). We previously showed that Cdh5Cre-mediated deletion of *Podxl* (*Podxl*$^{\Delta Cdh5Cre}$) (17) led to a modest leakage of plasma from circulation into the lung parenchyma, and that this effect was exacerbated in response to lipopolysaccharide (LPS)-induced lung inflammation, suggesting an underlying defect in lung microvascular integrity in the absence of Podxl on vECs (17). However, we were not able to detect any leakage defect in any other organ in naïve or LPS-induced *Podxl*$^{\Delta Cdh5Cre}$ mice.

Although *Podxl*$^{\Delta Cdh5Cre}$ mice delete Podxl efficiently in most vECs, they fail to delete Podxl in brain microvessels (23), likely due to the failure of the Cdh5 transgenic promoter elements to fully recapitulate the normal expression pattern of VE-cadherin in brain endothelia (25). Because Podxl is most highly expressed by these BBB endothelia (19), and because TJs and AJs play critical roles in the BBB's integrity to protect against immune-mediated

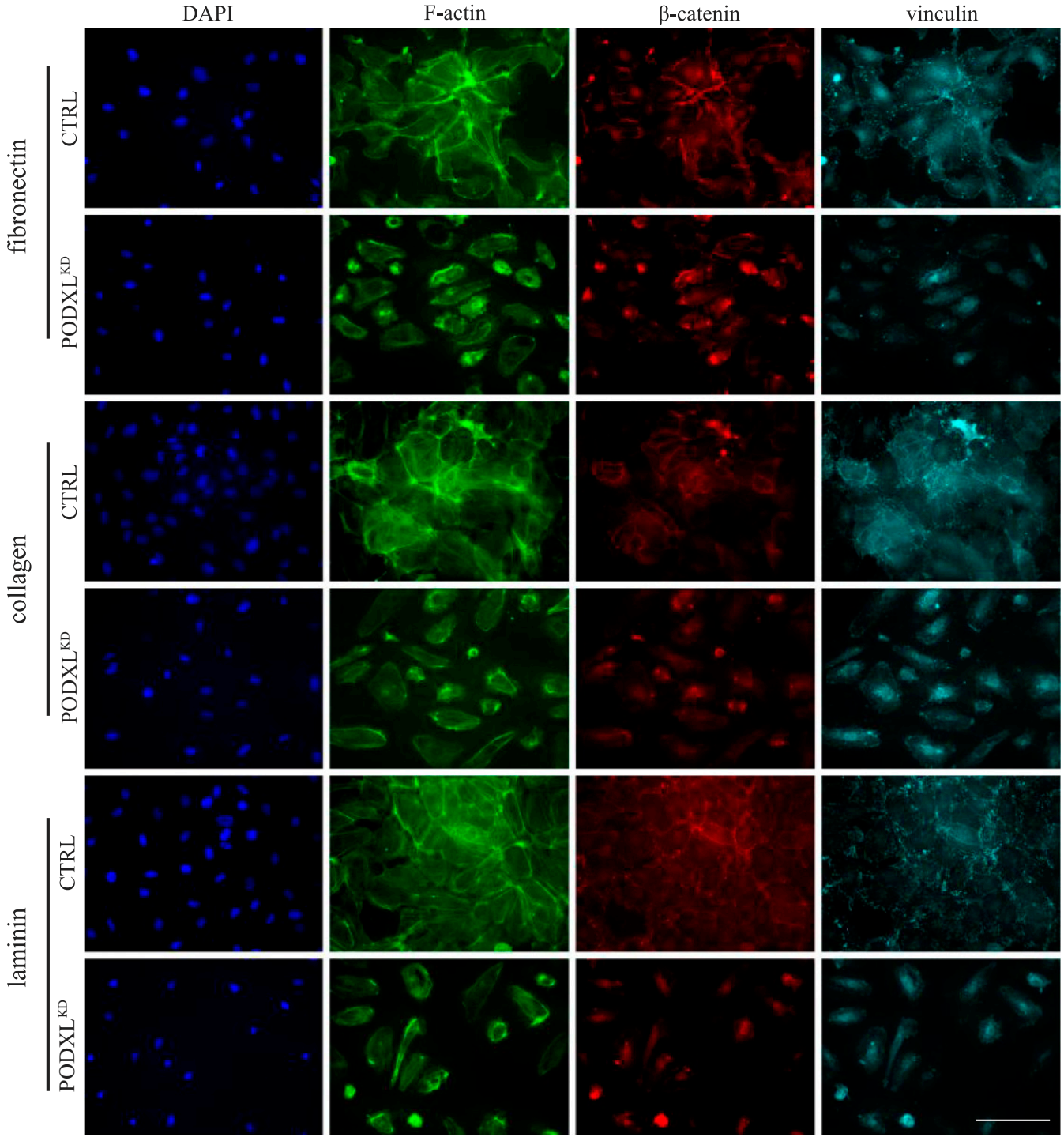

Fig. 2. Podxl expression in HUVECs is required for F-actin accumulation, association of β-catenin with cell junctions, and efficient formation of focal adhesion complexes. F-actin (phalloidin; green), β-catenin (red), and vinculin (aqua) staining of WT and PODXL^{KD} (KD) HUVECs at 72 h after seeding on the indicated matrix. DAPI (nuclear stain). (Scale bars: 100 μm.)

neural inflammation, we hypothesized that Podxl may selectively regulate BBB function. We and others have previously shown that the Tie2Cre strain is an efficient deleter of floxed genes in brain endothelia (*SI Appendix*, Fig. S5*F*); thus, we generated *Podxl*$^{\Delta Tie2Cre}$ mice to study Podxl function in the BBB. Following systemic administration of LPS, we injected mice with DyLight 649-coupled *Lycopersicon esculentum* (tomato) lectin (649-LEL) and Texas Red-coupled dextran (70 kDa) (TR-DEX$_{70}$) to mark the vascular endothelium and assess leakage of high molecular weight plasma components, respectively. LPS treatment selectively induces a robust accumulation of the TR-DEX$_{70}$ in the brain parenchyma of *Podxl*$^{\Delta Tie2Cre}$ but not wild-type (WT) mice (Fig. 4). This effect is not strictly linked to TLR4 signaling, since the TLR3 agonist polyinosinic:polycytidylic acid [poly(I:C)] elicits a similar response: Systemic administration of poly(I:C) induces the accumulation of TR-DEX$_{70}$ in the brain parenchyma

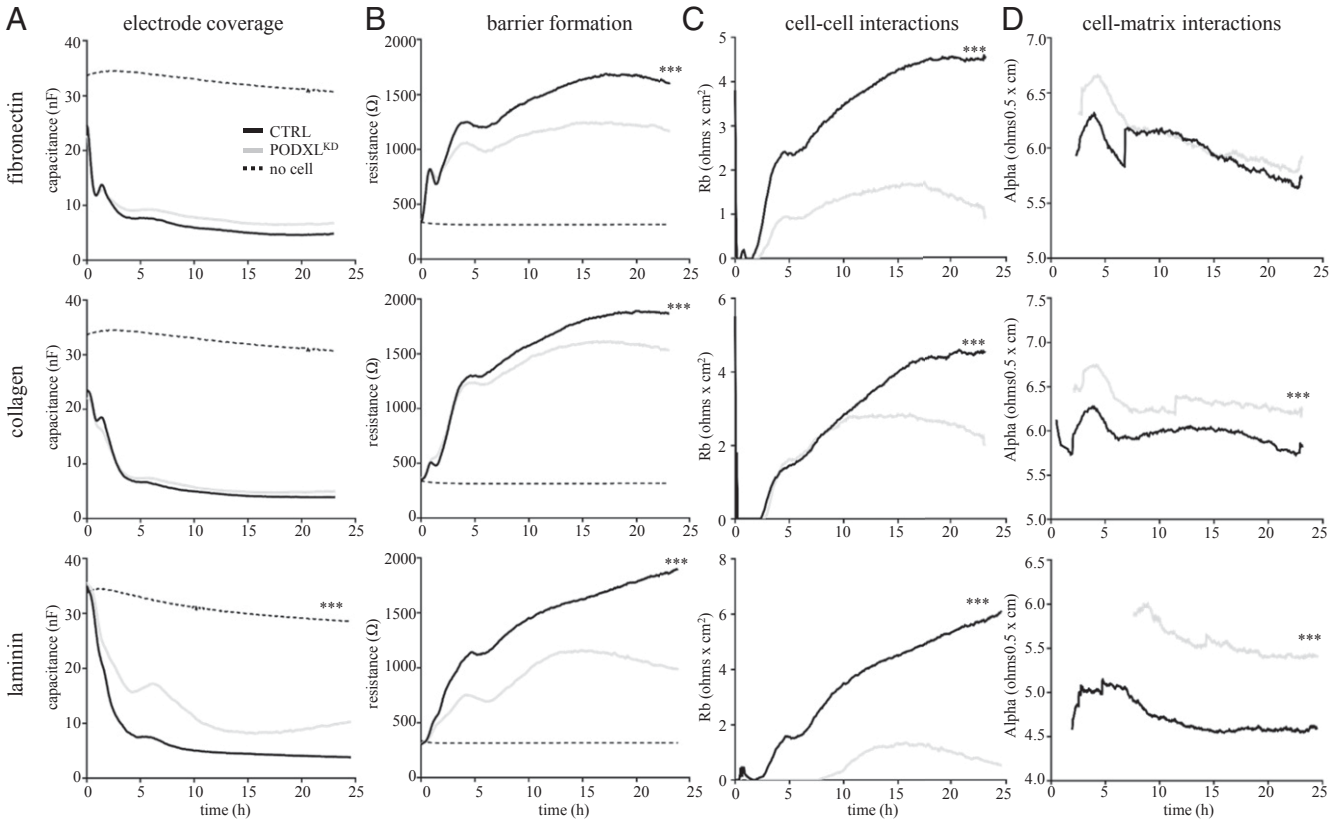

Fig. 3. Podxl promotes endothelial cell adhesion and barrier function. ECIS ZΘ assay of barrier function of control (scrambled siRNA; black line) and *PODXL* knockdown (PODXL^{KD}; gray line) HUVECs. Cell-free wells (dashed line) served as a negative control. Cells were seeded on matrix-coated 8W10E^{+} PET wells at a density of 1.5×10^5 cells/well. Electrode coverage and barrier parameters were measured at multiple frequencies (*f*). (*A*) Electrode coverage was measured as capacitance (nF) at 64 kHz. (*B*) Barrier formation was measured as resistance (W) at 4 kHz. (*C*) Modeling of cell–cell interactions (Rb). (*D*) Modeling of cell–matrix interactions (α). ***Significantly different from control with $P < 0.0001$ (determined by Student's *t* test) ($n = 3$ per condition).

of *Podxl*$^{\Delta Tie2Cre}$ but not WT mice (*SI Appendix*, Fig. S6). We did not observe TR-DEX$_{70}$ in the brain parenchyma in either WT or *Podxl*$^{\Delta Tie2Cre}$ naïve mice, suggesting that in the absence of inflammation, both strains are able to maintain appropriate homeostatic BBB integrity (Fig. 4). We conclude that although *Podxl*$^{\Delta Tie2Cre}$ mice appear to maintain normal BBB integrity under steady-state conditions, in response to systemic inflammation, Podxl is required for BBB maintenance.

A Selective PAR1-Agonist Peptide Induces Transient Suppression of Neuroelectric Activity in Podxl$^{\Delta Tie2Cre}$ Mice. Leakage of plasma constituents into the brain parenchyma propagates neuroinflammation and neurodegeneration (reviewed in ref. 26). At least part of this pathology is mediated by inappropriate exposure of the CNS parenchyma to plasma-restricted proteases, such as thrombin (27). Thrombin, a potent inducer of acute vascular permeability and platelet activation and aggregation (28), partly exerts its effects through a family of G protein-coupled protease activated receptors (PAR-1, -3, and -4) (29). In the mouse, PAR-1 is expressed on multiple cell types associated with the BBB neurovascular unit, including endothelial cells (30), glial cells (31, 32) and neurons (33). To more thoroughly assess the impact of disruption of the BBB in *Podxl*$^{\Delta Tie2Cre}$ mice, we treated mice with a selective PAR-1 agonist (TFLLR-NH$_2$) to (*i*) activate PAR-1 on vascular endothelia and disrupt barrier function (34) and (*ii*) determine whether the peptide agonist enters the CNS parenchyma to activate glia or neurons (33, 35–37).

We first primed mice with LPS for 6 h and then administered the PAR-1 agonist (i.v., tail vein) (Fig. 5*A*). Strikingly, the PAR-1 agonist induced an immediate loss of voluntary motor control in LPS-primed *Podxl*$^{\Delta Tie2Cre}$ mice (Fig. 5*B* and Movie S7) These mice became completely immobile for a period lasting an average of 5 min (Fig. 5*C*), followed by a rapid return to full activity and normal behavior. During the period of immobility, *Podxl*$^{\Delta Tie2Cre}$ mice retained ocular and pedal reflexes, normal respiration and heart rate, and normal tail vein blood pressure (*SI Appendix*, Fig. S7). Subsequent to their full recovery, *Podxl*$^{\Delta Tie2Cre}$ mice remained refractory to a second PAR-1 agonist treatment for at least 1 h, possibly reflecting receptor internalization or attenuation of signaling (38, 39). Poly(I:C) administration followed by the PAR-1 agonist also induced this immobility phenotype (Movie S8). None of the LPS-primed WT mice displayed a behavioral response to the PAR-1 agonist. Intriguingly, we found that PAR-1 agonist treatment did not significantly alter BBB permeability in WT or *Podxl*$^{\Delta Tie2Cre}$ mice above that previously observed with LPS alone (*SI Appendix*, Fig. S8) (40). Thus, we attribute the PAR-1–induced behavior of *Podxl*$^{\Delta Tie2Cre}$ mice to the ability of PAR-1 agonist to cross the BBB rather than an additional direct effect on LPS-primed endothelia.

To further confirm that the BBB leakage and behavior response to LPS and the PAR-1 agonist was selectively associated with deletion of Podxl from BBB vasculature, we performed similar experiments using *Podxl*$^{\Delta Cdh5Cre}$ mice. These mice delete *Podxl* from most vascular beds, with the notable exception of BBB endothelia, and thus served as an ideal control strain (17, 23, 24) (*SI Appendix*, Fig. S5). BBB integrity in LPS-primed *Podxl*$^{\Delta Cdh5Cre}$ mice was identical to WT mice (without the enhanced permeability seen in *Podxl*$^{\Delta Tie2Cre}$ mice; *SI Appendix*, Fig. S9), and, correspondingly, these mice failed to exhibit the same inertia response to PAR-1 agonist administration.

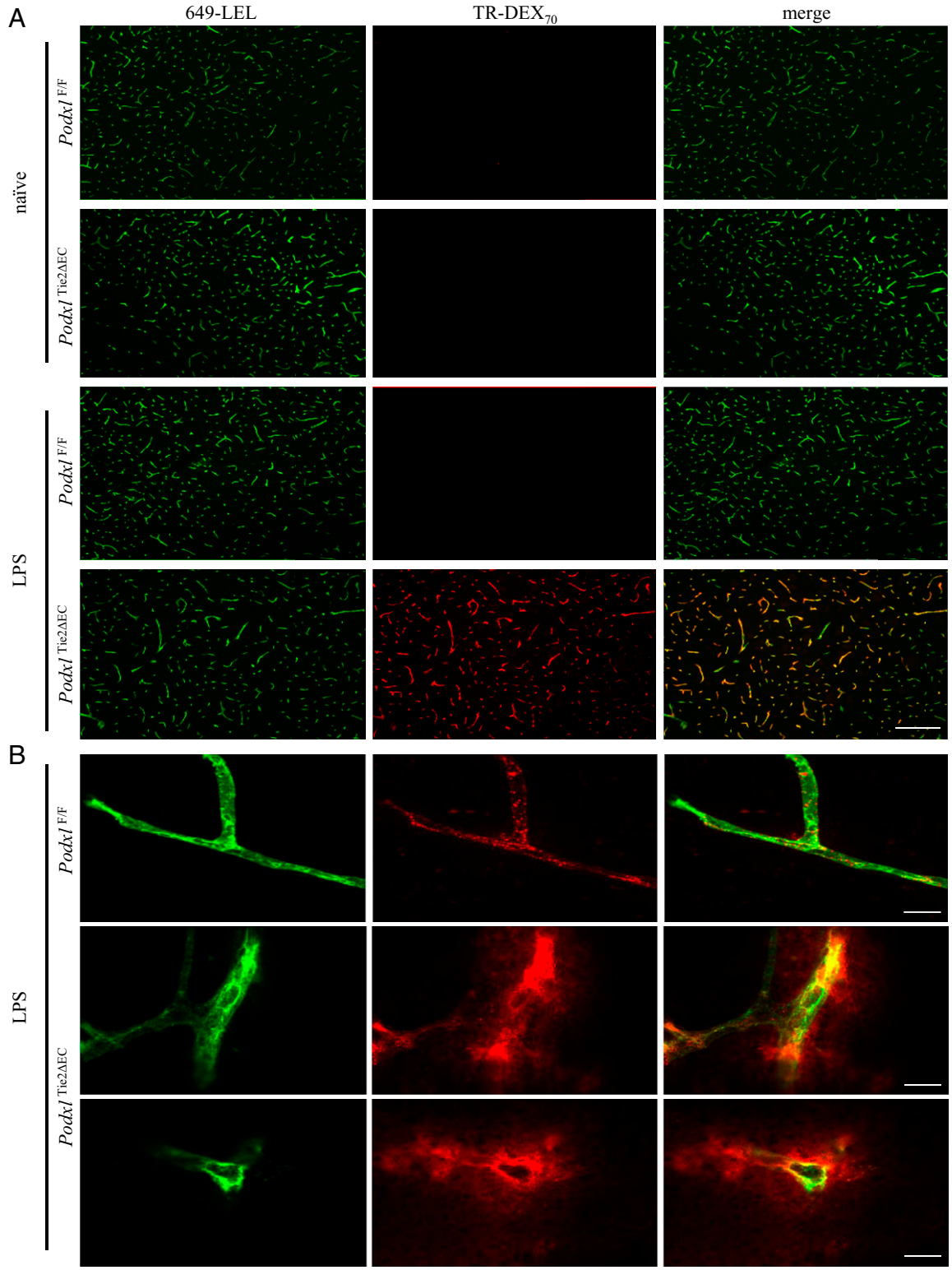

Fig. 4. Podxl expression in vascular endothelia promotes barrier function during LPS-induced inflammation. Fluorescence micrographs of the cerebral cortex region of brain harvested from naïve and LPS-treated (5 mg/kg i.p. for 6 h) mice. 649-LEL and TR-DEX$_{70}$ was circulated via the retro-orbital route to label vessel lumens and assess vascular barrier function. (*A*) Low-magnification images of perfused and fixed brain sections showing widespread perivascular dextran accumulation in *Podxl*$^{Tie2\Delta EC}$ mice. (Scale bars: 100 μm.) (*B*) Confocal images of nonperfused unfixed brains demonstrating extravasation of TR-DEX$_{70}$ from the blood vessel. *Podxl*$^{F/F}$ mouse showing the absence of TR-DEX$_{70}$ outside the vessel wall. *Podxl*$^{Tie2\Delta EC}$ mice showing presence of dextran clouds outside of the microvessel. (Scale bar: 10 μm.)

To further characterize the effects of the PAR-1 agonist on *Podxl*$^{\Delta Tie2Cre}$ mice, we recorded brain electrical activity by electroencephalography (EEG) in LPS-primed mice. We found that injection of the PAR-1 agonist induces a transient suppression of electrical activity that lasted roughly 5 min and corresponds closely with the period of observed inactivity (Fig. 5 *D* and *E*). In

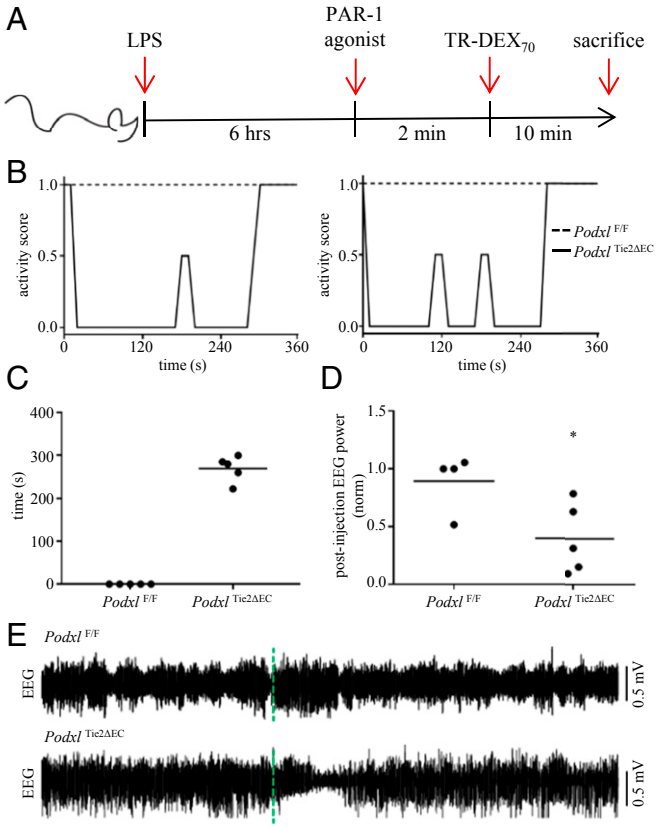

Fig. 5. A selective PAR-1 agonist peptide highlights the consequences of BBB dysfunction during neuroinflammation in LPS-primed *Podxl*$^{\Delta Tie2Cre}$ mice. (*A*) Overview of experimental model. (*B*) Relative activity levels of LPS-primed WT (*Podxl*$^{F/F}$) and *Podxl*$^{\Delta Tie2Cre}$ mice following administration of a selective PAR-1 agonist (5 mg/kg i.v.). Activity was scored by video review as follows: 1 = normal activity; 0.5 = subdued; 0 = no activity. Two examples are shown for each genotype. (*C*) Time (s) to recovery of full activity (score = 1). Videos of sample behavior can be viewed in Movie S7. (*D*) *Podxl*$^{\Delta Tie2Cre}$ mice exhibit suppression of EEG power (0.5–4 Hz) within 10 min after administration of PAR-1 agonist *Podxl*$^{\Delta Tie2Cre}$ = 39.9 ± 13.6% (n = 5 mice) vs. WT = 89.3 ± 12.6% (n = 4 mice) of preinjection baseline EEG power ($P < 0.05$, Student's t test). Data points represent measurements from individual mice and the horizontal lines represent means. (*E*) Example EEG recordings of spontaneous activity from a surface electrode placed near the primary somatosensory cortex in LPS-primed *Podxl*$^{\Delta Tie2Cre}$ and WT mice following administration of PAR-1 agonist (5 mg/kg i.v.). The time of PAR-1 agonist administration (t = 0) is indicated with a dashed green line.

summary, although *Podxl*-deficient vECs appear capable of forming functional endothelial barriers in vivo, they exhibit a striking inability to maintain and/or reform these in response to acute inflammation, leading to enhanced brain exposure to serum components normally excluded from the CNS parenchyma (Fig. 6).

Discussion

Podxl was one of the first identified markers of the apical membrane domains of polarized epithelial cells. However, its function remains highly controversial, with evidence suggesting that it can participate in both proadhesive and antiadhesive processes (14, 41, 42). More recently, both gene deletion and overexpression studies have suggested that Podxl's primary function is to facilitate formation of appropriately positioned "preapical" and basolateral domains and the appropriate localization of cell–cell and cell–matrix adhesion complexes (16, 18, 43). Thus, although the negatively charged mucin domain serves to prevent nonspecific cell adhesion, Podxl also facilitates the segregation and exclusion of integrins and junctional proteins from apical domains and aids in their appropriate targeting to basolateral membranes. Thus, Podxl can also enhance cell adhesion to matrix and neighboring cells. This dual function—blocking apical adhesion while facilitating junction and adhesion molecule localization and positioning—likely explains why Podxl appears to facilitate adhesion in some scenarios and block adhesion in others (41).

Here we found that Podxl expression in HUVECs promotes the maintenance of cell–cell contacts and cell–matrix adhesion interactions. Although both control and PODXL^{KD} cells are able to initially generate dense monolayers, over time in the absence of Podxl, monolayers become progressively disrupted regardless of the ECM on which they attempt to adhere. Furthermore, we find that suppression of Podxl expression results in mislocalization of FA and AJ complexes in HUVECs. Although monolayer formation appears normal during the first 24 h, light microscopy and real-time ECIS analyses demonstrate that Podxl is required for the optimal formation of electrically resistant barriers. Despite initial normal cell spreading and growth characteristics (electrode coverage) on fibronectin and collagen, defects in barrier formation are detected (electrical resistance) on all matrices. Differences in electrical resistance are most striking on laminin, where Podxl plays a key role in endothelial cell spreading. Thus, consistent with previous observations with epithelial cell lines and highly specialized primary epithelia (podocytes), our data argue that in primary vascular endothelia Podxl plays critical roles in proper segregation of apical and basolateral membrane structures and targeting of adhesion complexes.

Intriguingly, although Podxl loss cripples the ability of endothelial cells to form appropriate intact monolayers in vitro, we observed no overt severe vascular defects due to Podxl loss in vivo at steady state. *Podxl*-deficient mice exhibited only a modest delay in the opening of vascular lumens during embryogenesis and a modest increase in permeability in adulthood (17, 44, 45). Thus, in vivo there appear to be sufficiently redundant mechanisms to ensure appropriate formation of properly patent vessels to allow survival in the absence of Podxl. This could occur through several mechanisms; the ECM milieu in vivo is far more complex than the single components tested in vitro. Likewise, the stiffness of the plastic substratum in vitro fails to adequately mimic the more compliant substratum in vivo.

Finally, because Podxl is but one member of a large family of endothelial sialomucins, one or more of these additional proteins could be up-regulated to functionally compensate during steady-state homeostasis in vivo but fail to support integrity in response to stress. Likewise, the acute knockdown of Podxl in HUVECs in vitro might not provide adequate time for engagement of these compensatory mechanisms. It is also noteworthy that CD34, Podxl's closest relative, undergoes a striking down-regulation over the first 96 h of HUVEC culture in vitro, which would in principal preclude its ability to act as a compensatory molecule in vitro (46). Future experiments using Podxl/CD34 double-deficient mice may offer an opportunity to clarify whether this is a valid salvage pathway in vivo.

Despite the normal phenotype of Podxl mice at steady state, we reasoned that vascular function might be compromised in situations of acute stress, and thus examined the vascular function of Podxl in maintenance of the BBB, the endothelial structure in which it is most highly expressed (19). Strikingly, we found that Podxl loss compromises the ability of the BBB to maintain integrity in response to LPS-induced inflammation. The thrombin receptor PAR-1 is highly expressed by cells comprising the neurovascular unit in mouse and human CNS (36). Agonism of PAR-1 has been proposed to promote vascular barrier disruption in vECs, and its activation in neural tissue has been shown to promote survival of neurons and to regulate both neurodegeneration and neuroprotection in various experimental

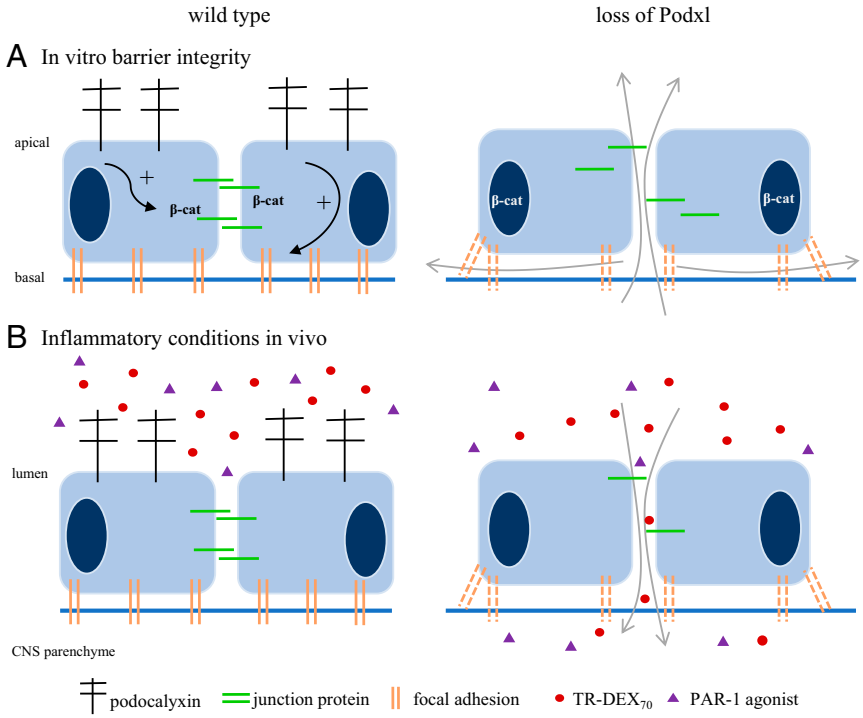

Fig. 6. Proposed model for Podxl's function in endothelial barrier formation and BBB maintenance during acute inflammation. (*A*, *Left*) On control endothelial cells, Podxl is expressed on the apical face. Expression of Podxl promotes formation and/or localization of focal adhesions to the basal matrix and stabilization of junctional complexes at cell–cell contacts. β-cat, beta-catenin. (*A*, *Right*) Suppression of Podxl expression leads to mislocalization of adhesion complexes and disorganization of focal adhesions. These defects disrupt cell–cell and cell–matrix barrier function (arrows). (*B*) Administration (i.p.) of LPS induces acute systemic inflammation in mice. (*Left*) In WT mice, Podxl stabilizes cell–cell junctions and matrix adhesion to maintain BBB function during acute inflammation. The BBB remains impermeable to serum components, including administered PAR-1 agonist or TR-DEX_{70}. (*Right*) In the absence of Podxl, acute inflammation disrupts the BBB sufficiently to allow entry of serum components. Thus, in the absence of Podxl expressed on brain endothelia, polar peptides like the PAR-1 agonist (TFLLR-NH_2) and large molecules (TR-DEX_{70}) can enter the CNS parenchyma, with potential neurologic consequences.

models of stroke and brain injury (47). When activated on astrocytes, PAR-1 regulates glutamatergic signaling (48). Although we did not observe an enhanced effect of PAR-1 agonists on vascular permeability in the present study, we found that it induced a transient suppression of EEG-detected electrical activity and a loss of motor function in LPS-primed *Podxl*$^{\Delta Tie2Cre}$ but not WT mice. The remarkably consistent 5-min period of immobility was followed by a full recovery. This behavior may be similar to the "freezing" behavior observed in rats after an NMDA-induced cortical spreading depression (49). Transient suppression of EEG activity can be observed following a cortical spreading depression, which can be triggered following an ischemic episode, acute injury, or excitotoxic insult (50). We propose that active neuroinflammation (e.g., LPS treatment) in *Podxl*$^{\Delta Tie2Cre}$ mice permits entry of a selective PAR-1 agonist peptide into the brain parenchyma, leading to a transient suppression of cerebral cortex electrical activity. Since this pathology is only observed in mice lacking Podxl on the brain endothelia, and not in mice lacking Podxl on other vascular beds, these data suggest a selective role for Podxl in BBB function. Accordingly, we propose that Podxl has a critical neuroprotective role through maintenance of BBB integrity during acute neuroinflammation.

Podxl's regulation of stress-induced BBB vascular integrity has interesting therapeutic implications. BBB function is critical to the healthy function of the CNS. Hyperpermeability of this barrier is known to contribute to the pathology of various acute inflammatory diseases, including traumatic brain injury and stroke. Similarly, in chronic neurodegenerative diseases, including multiple sclerosis, amyotrophic lateral sclerosis, Parkinson's disease, meningitis, and Alzheimer's disease, accumulating evidence suggests declining BBB integrity is a harbinger of poor outcome or even an initiating insult. Thus, enhancing Podxl-dependent integrity may prove therapeutic in both acute and chronic diseases. Alternatively, a major hindrance to therapeutic drug delivery to the CNS is the inability of most agents to cross the BBB. Thus, a transient down-modulation of Podxl-dependent BBB integrity could offer an opportunity for transient drug delivery.

Methods

HUVEC Tissue Culture. HUVECs were harvested from umbilical cords supplied by donors with informed consent (Human Ethics no. H10-00643). HUVECs were maintained at 37 °C, high humidity, and 5% CO_2 and used between passages 2 and 8.

siRNA Silencing of Podxl in HUVECs. Suppression of Podxl expression was achieved by transfecting HUVECs overnight with *PODXL* targeting or scrambled control siRNA using oligofectamine transfection reagent (Life Technologies; catalog no. 12252011). Knockdown of cell surface-expressed Podxl protein was confirmed by flow cytometry. Control and Podxl knockdown (PODXL^{KD}) HUVECs were subsequently used for experiments for up to 4 d posttransfection.

Barrier Function Assay. ECIS arrays (8W10E+ PET; Applied BioPhysics) were stabilized using cysteine buffer and then coated with fibronectin (10 μg/mL; Sigma-Aldrich, catalog no. F1141), laminin (5 μg/mL; R&D Systems, catalog no. 3400–010-01), collagen (1% gelatin; Sigma-Aldrich) or left uncoated. Then 1.5×10^5 cells were seeded into eight-well arrays, and resistance and capacitance were continuously measured for 24 h at multiple frequencies (*f*) on the ECIS ZΘ instrument (Applied BioPhysics). Resistance (barrier function) was continuously monitored for 24 h at 4,000 Hz. Capacitance (electrode coverage) was assessed at 64,000 Hz (22, 51). Rb (cell–cell interactions) and α (cell–matrix interactions) parameters were calculated using Applied Biophysics mathematical modeling (21).

Video Microscopy. HUVECs (3×10^5 cells/well) were plated in 48-well tissue culture-treated plastic plates coated with ECM components (fibronectin, 10 μg/mL; laminin, 5 μg/mL; collagen, 1% gelatin) as indicated in the figures. Cultures were then imaged every 3 h for 4 d using IncuCyte Zoom instrumentation and software.

Monolayer Assessment. HUVECs were lifted with 0.025% trypsin, counted, and plated at identical cell densities on glass coverslips coated with fibronectin, laminin (NeuVitro GG-12), or collagen (1% gelatin). At the endpoint of the experiment, cells were washed and fixed in 4% paraformaldehyde (Electron Microscopy Sciences) in PBS for 10 min on ice. For immunofluorescence microscopy, cells were stained with Alexa Fluor 488 phalloidin (A12379; Life Technologies), anti-vinculin (V9264; Sigma-Aldrich), anti–β-catenin (9562S; Cell Signaling Technology), or anti–VE-cadherin (2500S; Cell Signaling Technology) antibodies. Cells were mounted with Prolong Gold Antifade containing DAPI (P36935; Life Technologies). Imaging was performed using a Nikon Eclipse Ni-U epifluorescence microscope. Image analysis was performed using ImageJ.

Mice. Tie2-Cre mice [B6.Cg-Tg(Tek-Cre)12Flv/J] were obtained from The Jackson Laboratory (JAX #004128). B6-congenic (Cg) conditional Podxl KO ($Podxl^{F/F}$) (17) were crossed with Tie2-Cre to delete Podxl specifically in the vascular endothelial tissue strain ($Podxl^{\Delta Tie2Cre}$). $Podxl^{\Delta Tie2Cre}$ (B6-Cg) were described previously (17). All mice were maintained under specific pathogen-free conditions at the Biomedical Research Centre. Experiments were performed humanely based on recommendations of the Canadian Committee on Animal Care with approval of the University of British Columbia's Animal Care Committee (A14-0269, to K.M.M. and A18-0036, to T.H.M.).

Animal Model of BBB Permeability. LPS (LPS-EK; Invivogen) prepared in PBS (1 mg/mL) was administered to mice at 5 mg/kg via i.p. injections. After 6 h, LPS- (or PBS-) treated mice were killed for analysis as described below or, in some experiments, treated with 5 mg/kg PAR-1 agonist (TFLLR-NH_2, SCP0237; Sigma-Aldrich) prepared in PBS or PBS alone (i.v., tail vein). Mice treated with the PAR-1 agonist were observed for changes in behavior and video recorded for subsequent analysis. Mice treated with PBS did not demonstrate any change in activity. Activity was scored by reviewing videos based on total motion observed at 10-s intervals (with 1 = normal, 0.5 = reduced activity, and 0 = no activity) and time for fully recovery (sustained return to a score of 1).

In Vivo Immunofluorescence. Control mice and mice treated with LPS and/or the PAR-1 agonist (as indicated in the figures) were anesthetized with 2,2,2-tribromoethanol followed by retro-orbital administration of Texas red (TR) dextran 70 kDa (TR-DEX_{70}, D1864; Thermo Fisher Scientific), 125 μg/mouse, mixed with DyLight 649-labeled *L. esculentum* (tomato) lectin (649-LEL, 50 μg/mouse; DL1178; Vector Laboratories) in a 100-μL total volume. The TR-DEX_{70} and 649-LEL mixture was allowed to circulate for 10 min, after which mice were perfused with PBS followed by 10% formalin (10 mL each) through the cardiac right ventricle. Skulls were removed and postfixed in 4% paraformaldehyde at 4 °C for 24 h. The brains were removed and paraffin embedded. Brain sections (10 μm) were cut, rehydrated, mounted, and imaged by fluorescence microscopy to assess vascular permeability. Imaging was performed using a Nikon Eclipse Ni-U epifluorescence microscope. Image analysis was performed using ImageJ.

Confocal Immunofluorescence of Dextran Presence. LPS-treated mice were anesthetized with 2,2,2-tribromoethanol, followed by retro-orbital administration of TR-DEX_{70} (Thermo Fisher Scientific), 125 μg/mouse, mixed with DyLight 649-labeled *L. esculentum* (tomato) lectin (649-LEL, DL1178; Vector Laboratories), 50 μg/mouse, in 100 μL of total volume. The TR-DEX_{70} and 649-LEL mixture was allowed to circulate for 10 min. Tissue was prepared as described previously (52). In brief, anesthetized mice were placed on ice and immediately decapitated. Fresh brain tissue was snap-frozen in OCT. Brain sections (30 μm) were cut, mounted, and imaged immediately to assess vascular permeability by fluorescence microscopy. Imaging was performed by confocal microscopy (Zeiss LSM 800 with Ariyscan). Image analysis was performed using ImageJ.

EEG. $Podxl^{\Delta Tie2Cre}$ and $Podxl^{F/F}$ (WT) mice were induced with isoflurane anesthesia (1% maintenance mixed with oxygen), and body temperature was maintained at 37 °C using a heating pad and feedback regulation from a rectal temperature probe. A craniotomy was performed over the right somatosensory cortex, and the skull was fastened to a stainless-steel plate with cyanoacrylate glue and dental cement. A Teflon-coated, chloridized silver wire (0.125 mm) was placed on the right edge of the craniotomy. A reference electrode was placed on the nasal bone. The cortical signal was amplified (1,000×) and filtered (0.1–1,000 Hz) using an AM Systems model 1700 AC amplifier and digitized using a 1322A Digidata digitizer.

1. Wallez Y, Huber P (2008) Endothelial adherens and tight junctions in vascular homeostasis, inflammation, and angiogenesis. *Biochim Biophys Acta* 1778:794–809.
2. Wu MH (2005) Endothelial focal adhesions and barrier function. *J Physiol* 569: 359–366.
3. Becker BF, Chappell D, Jacob M (2010) Endothelial glycocalyx and coronary vascular permeability: The fringe benefit. *Basic Res Cardiol* 105:687–701.
4. Lai CH, Kuo KH, Leo JM (2005) Critical role of actin in modulating BBB permeability. *Brain Res Brain Res Rev* 50:7–13.
5. Tietz S, Engelhardt B (2015) Brain barriers: Crosstalk between complex tight junctions and adherens junctions. *J Cell Biol* 209:493–506.
6. Ben Shimon M, et al. (2015) Thrombin regulation of synaptic transmission and plasticity: Implications for health and disease. *Front Cell Neurosci* 9:151.
7. Doyonnas R, et al. (2005) Podocalyxin is a CD34-related marker of murine hematopoietic stem cells and embryonic erythroid cells. *Blood* 105:4170–4178.
8. Sathyanarayana P, et al. (2007) Erythropoietin modulation of podocalyxin and a proposed erythroblast niche. *Blood* 110:509–518.
9. Maltby S, Hughes MR, Zbytnuik L, Paulson RF, McNagny KM (2009) Podocalyxin selectively marks erythroid-committed progenitors during anemic stress but is dispensable for efficient recovery. *Exp Hematol* 37:10–18.
10. Snyder KA, et al. (2015) Podocalyxin enhances breast tumor growth and metastasis and is a target for monoclonal antibody therapy. *Breast Cancer Res* 17:46.
11. McNagny KM, et al. (2012) Podocalyxin in the diagnosis and treatment of cancer. *Advances in Cancer Management*, ed PRM InTech (IntechOpen Limited, London), pp 155–194.
12. Schnabel E, Dekan G, Miettinen A, Farquhar MG (1989) Biogenesis of podocalyxin—the major glomerular sialoglycoprotein—in the newborn rat kidney. *Eur J Cell Biol* 48: 313–326.
13. Kerjaschki D, Vernillo AT, Farquhar MG (1985) Reduced sialylation of podocalyxin—the major sialoprotein of the rat kidney glomerulus—in aminonucleoside nephrosis. *Am J Pathol* 118:343–349.
14. Doyonnas R, et al. (2001) Anuria, omphalocele, and perinatal lethality in mice lacking the CD34-related protein podocalyxin. *J Exp Med* 194:13–27.
15. Kang HG, et al. (2017) Loss of podocalyxin causes a novel syndromic type of congenital nephrotic syndrome. *Exp Mol Med* 49:e414.
16. Nielsen JS, et al. (2007) The CD34-related molecule podocalyxin is a potent inducer of microvillus formation. *PLoS One* 2:e237.
17. Debruin EJ, et al. (2014) Podocalyxin regulates murine lung vascular permeability by altering endothelial cell adhesion. *PLoS One* 9:e108881, and erratum (2014) 9: e116613.
18. Bryant DM, et al. (2014) A molecular switch for the orientation of epithelial cell polarization. *Dev Cell* 31:171–187.
19. Agarwal N, Lippmann ES, Shusta EV (2010) Identification and expression profiling of blood-brain barrier membrane proteins. *J Neurochem* 112:625–635.
20. Xu J, Shi GP (2014) Vascular wall extracellular matrix proteins and vascular diseases. *Biochim Biophys Acta* 1842:2106–2119.
21. Lo CM, Keese CR, Giaever I (1999) Cell-substrate contact: Another factor may influence transepithelial electrical resistance of cell layers cultured on permeable filters. *Exp Cell Res* 250:576–580.
22. Giaever I, Keese CR (1991) Micromotion of mammalian cells measured electrically. *Proc Natl Acad Sci USA* 88:7896–7900.
23. Alva JA, et al. (2006) VE-cadherin-Cre-recombinase transgenic mouse: A tool for lineage analysis and gene deletion in endothelial cells. *Dev Dyn* 235:759–767.
24. Kisanuki YY, et al. (2001) Tie2-Cre transgenic mice: A new model for endothelial cell-lineage analysis in vivo. *Dev Biol* 230:230–242.
25. Hisatsune H, et al. (2005) High level of endothelial cell-specific gene expression by a combination of the 5′ flanking region and the 5′ half of the first intron of the VE-cadherin gene. *Blood* 105:4657–4663.
26. Carvey PM, Hendey B, Monahan AJ (2009) The blood-brain barrier in neurodegenerative disease: A rhetorical perspective. *J Neurochem* 111:291–314.
27. Armao D, Kornfeld M, Estrada EY, Grossetete M, Rosenberg GA (1997) Neutral proteases and disruption of the blood-brain barrier in rat. *Brain Res* 767:259–264.
28. Macfarlane SR, Seatter MJ, Kanke T, Hunter GD, Plevin R (2001) Proteinase-activated receptors. *Pharmacol Rev* 53:245–282.
29. Alberelli MA, De Candia E (2014) Functional role of protease-activated receptors in vascular biology. *Vascul Pharmacol* 62:72–81.
30. Connolly TM, et al. (1994) Species variability in platelet and other cellular responsiveness to thrombin receptor-derived peptides. *Thromb Haemost* 72:627–633.
31. Kataoka H, et al. (2003) Protease-activated receptors 1 and 4 mediate thrombin signaling in endothelial cells. *Blood* 102:3224–3231.
32. Boven LA, et al. (2003) Up-regulation of proteinase-activated receptor 1 expression in astrocytes during HIV encephalitis. *J Immunol* 170:2638–2646.

33. Balcaitis S, et al. (2003) Expression of proteinase-activated receptors in mouse microglial cells. *Neuroreport* 14:2373–2377.
34. Kaneider NC, et al. (2007) "Role reversal" for the receptor PAR1 in sepsis-induced vascular damage. *Nat Immunol* 8:1303–1312.
35. Han KS, et al. (2011) Activation of protease activated receptor 1 increases the excitability of the dentate granule neurons of hippocampus. *Mol Brain* 4:32.
36. Junge CE, et al. (2004) Protease-activated receptor-1 in human brain: Localization and functional expression in astrocytes. *Exp Neurol* 188:94–103.
37. Striggow F, et al. (2001) Four different types of protease-activated receptors are widely expressed in the brain and are up-regulated in hippocampus by severe ischemia. *Eur J Neurosci* 14:595–608.
38. Gur-Cohen S, et al. (2015) PAR1 signaling regulates the retention and recruitment of EPCR-expressing bone marrow hematopoietic stem cells. *Nat Med* 21:1307–1317.
39. Soh UJ, Dores MR, Chen B, Trejo J (2010) Signal transduction by protease-activated receptors. *Br J Pharmacol* 160:191–203.
40. Kawabata A, et al. (1999) Enhancement of vascular permeability by specific activation of protease-activated receptor-1 in rat hindpaw: A protective role of endogenous and exogenous nitric oxide. *Br J Pharmacol* 126:1856–1862.
41. Nielsen JS, McNagny KM (2008) Novel functions of the CD34 family. *J Cell Sci* 121:3683–3692.
42. Sassetti C, Tangemann K, Singer MS, Kershaw DB, Rosen SD (1998) Identification of podocalyxin-like protein as a high endothelial venule ligand for L-selectin: Parallels to CD34. *J Exp Med* 187:1965–1975.
43. Meder D, Shevchenko A, Simons K, Füllekrug J (2005) Gp135/podocalyxin and NHERF-2 participate in the formation of a preapical domain during polarization of MDCK cells. *J Cell Biol* 168:303–313.
44. Strilić B, et al. (2009) The molecular basis of vascular lumen formation in the developing mouse aorta. *Dev Cell* 17:505–515.
45. Horrillo A, Porras G, Ayuso MS, González-Manchón C (2016) Loss of endothelial barrier integrity in mice with conditional ablation of podocalyxin (Podxl) in endothelial cells. *Eur J Cell Biol* 95:265–276.
46. Delia D, et al. (1993) CD34 expression is regulated reciprocally with adhesion molecules in vascular endothelial cells in vitro. *Blood* 81:1001–1008.
47. Luo W, Wang Y, Reiser G (2007) Protease-activated receptors in the brain: Receptor expression, activation, and functions in neurodegeneration and neuroprotection. *Brain Res Brain Res Rev* 56:331–345.
48. Sweeney AM, et al. (2017) PAR1 activation induces rapid changes in glutamate uptake and astrocyte morphology. *Sci Rep* 7:43606.
49. Akcali D, Sayin A, Sara Y, Bolay H (2010) Does single cortical spreading depression elicit pain behaviour in freely moving rats? *Cephalalgia* 30:1195–1206.
50. Lauritzen M, et al. (2011) Clinical relevance of cortical spreading depression in neurological disorders: Migraine, malignant stroke, subarachnoid and intracranial hemorrhage, and traumatic brain injury. *J Cereb Blood Flow Metab* 31: 17–35.
51. Szulcek R, Bogaard HJ, van Nieuw Amerongen GP (2014) Electric cell-substrate impedance sensing for the quantification of endothelial proliferation, barrier function, and motility. *J Vis Exp,* 85.
52. Hoffmann A, et al. (2011) High and low molecular weight fluorescein isothiocyanate (FITC)-dextrans to assess blood-brain barrier disruption: Technical considerations. *Transl Stroke Res* 2:106–111.